

# A Novel Wind Turbine System Using NPC Topology- Back To Back Converter by Open-Switch Fault Detection Method

K. Kavitha<sup>1</sup>, P. Srinivasan<sup>2</sup>PG Scholar, Dept. of EEE, SRM University, Chennai, Tamilnadu, India<sup>1</sup>Asst. Prof, Dept. of EEE, SRM University, Chennai, Tamilnadu, India<sup>2</sup>

**ABSTRACT:** In this paper using Back to back converters transfer power from permanent magnet synchronous generator to grid. A back to back converter with neutral point clamped topology is widely used. There are 12 switches is NPC(Neutral point clamped) topology. Open switch fault in NPC rectifier or back to back converter leads to distortion of input current. Open switch fault in NPC inverter of back to back converter leads to distortion of output current. An open switch fault causes a change in current pattern and can cause breakdown of other parts. Hence detection of open switch fault prevents the destruction of other components and improves reliability of the system.

**KEYWORDS:** Permanent magnet, NPC rectifier, NPC inverter and open switch fault.

## I. INTRODUCTION

Most of the countries in the world use coal, oil, and natural gas to supply most of their energy needs. As world population continues to grow and the limited amounts of fossil fuels begin to diminish, it may not be possible to provide the amount of energy demanded by the world by only using fossil fuels. Burning fossil fuels to convert the energy also creates air, water, and soil pollution. In addition, it produces greenhouse gases which are responsible for the global warming. There are plenty of ways to convert the energy without fossil fuels like renewable energy. Renewable energy resources such as wind, solar, and hydropower offer clean alternatives to fossil fuels. Among them, the wind power is a cost-effective, efficient, and abundant source of electricity. For this reason, the wind industry has been growing rapidly in recent years to

reduce the global warming and the dependence on fossil fuels. Wind energy conversion system (WECS) is generally composed of a wind turbine, an electric generator, a generator-side converter and a grid-side inverter. Different structures for a WECS can be realized to convert the wind energy at varying wind speeds to electric power. The most advanced generator type is the permanent magnet synchronous generator (PMSG) used for variable speed wind power generation systems.

Generally, power switch failures can be classified as short-switch fault and open switch fault. Short-switch faults are produced by gate circuit degradation and AC overcurrent. A short-switch fault generates an unbalanced over current, which causes damage in other important devices of the system. The unbalanced over voltage and over current may result in fatal accidents. Therefore, such a fault should be detected immediately to protect expensive devices. There are several reasons that cause an open-switch fault. The open-switch faults are created by the disconnection of a wire from the switching devices

due to a thermal cycling or a gate driver failure. Open-switch faults may be caused by high collector current. Finally, the failure in gate driver circuits is one of the most common causes of open-switch fault. Although open-switch faults do not cause the

shutdown of the entire system, the performance will be degraded. Also, the unbalanced operation caused by the open-switch faults may generate secondary problems in the system. When any power switch presents state of failure in a generator-side converter or in a grid-side inverter, the other components of the system can be damaged. For this reason, open-switch faults should be detected as soon as the fault occurs. It is very important to identify the location of faulty

# International Journal of Innovative Research in Science, Engineering and Technology

(An ISO 3297: 2007 Certified Organization)

Vol. 5, Issue 3, March 2016

switch properly. If any kinds of open-switch faults occur either in a generator-side converter or in a grid-side inverter, the energy supplied to the grid will be reduced continuously. Diagnostic methods for the open-switch fault in an AC/DC PWM converter have been developed with a special focus on condition monitoring [1]. The difference in detection methods between three-phase AC/DC PWM converter and inverter has been analyzed for IGBT open-switch faults [2]. Based on these techniques, an alternative fault detection method has been proposed for the PWM inverter. A new voltage-based approach without additional sensors has been proposed for open-switch fault diagnosis in closed loop controlled PWM voltage source converter [3]. In this scheme, the information contained in the reference voltages which are available from the controller has been used as detection variables. Four detection techniques using various voltage informations have been introduced for fault diagnosis in voltage-fed asynchronous machine drive systems [4]. Application of the fuzzy logic for a fault diagnosis of switching device in a voltage fed induction motor was presented in [5].

A survey was done on the existing methods of fault diagnosis and protection of IGBT [6]. A real-time diagnosis for multiple open-switch faults in voltage-fed PWM motor drives was proposed in [7, 8]. Open-switch fault diagnosis of AC/DC PWM converter has become essential in wind turbine applications, not only to avoid secondary fault in the AC/DC PWM converter but also to improve the stability and reliability of entire system. A diagnostic method for multiple open-switch faults in the two converters of a PMSG drive has been proposed for wind turbine applications [9]. A diagnostic method for a doubly-fed wind power converter in microgrid system has been presented [10], which is based on the investigation of the characteristics of current signals. A system reconfiguration topology was designed for the microgrid system to keep a doubly-fed induction generator continue running after the open-switch faults. A fault diagnosis method based on the analysis of the load currents in voltage source inverters was proposed [11], which was an extension of the normalized dc components method. By combining the normalized dc components with additional diagnostic variables, the certainty of the diagnoses under transients and light loads has been markedly improved. Since the performance and reliability of the system are degraded due to the open switch fault, a fault tolerant control method is needed to solve this problem. A fault diagnostic method and fault tolerant topology have been proposed for the generator-side converter [12] to minimize the unbalance of AC input current and the ripple voltage in the DC-link of three-phase AC/DC PWM converter. Fault detection and isolation on a PWM inverter using the knowledge based model were investigated [13]. This scheme was based on the analysis of the current vector trajectory and instantaneous frequency in faulty mode and validated through the simulations and experiments. Some diagnostic methods use the fuzzy theory and model reference adaptive system [14]. In this study, the simulations and experiments were carried out for a digitally controlled permanent magnet synchronous motor drive system to show the effectiveness and simplicity. A fault diagnostic technique to detect the fault type and fault location in multilevel inverter has been also proposed and validated [15]. A novel fast diagnostic method for open-switch faults in inverters without sensors has been proposed [16] to improve the reliability of the system. This scheme is achieved by the analysis using switching function model of inverter under both healthy and faulty conditions.

## II. PROPOSED FAULT DETECTION METHOD

A flow chart of the proposed fault detection algorithm is presented in Figure 1. In the proposed fault detection algorithm, three-phase voltages  $V_a$ ,  $V_b$ , and  $V_c$  are calculated at first by using the DC link voltage and switching times from the space vector PWM scheme.

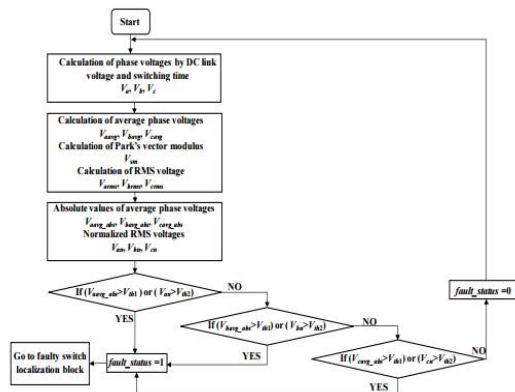


**Fig. 1 Flow Chart of the Proposed Open-Switch Fault Detection Algorithm**

From these values, the absolute values of average three-phase voltages  $V_{avg\_abs}$ ,  $V_{bavg\_abs}$ , and  $V_{cavg\_abs}$  and the normalized three-phase RMS voltages  $V_{an}$ ,  $V_{bn}$ , and  $V_{cn}$  are calculated by using three-phase RMS voltages and Park's vector modulus. The switching pattern in the symmetrical space vector PWM scheme is shown in Figure 2.

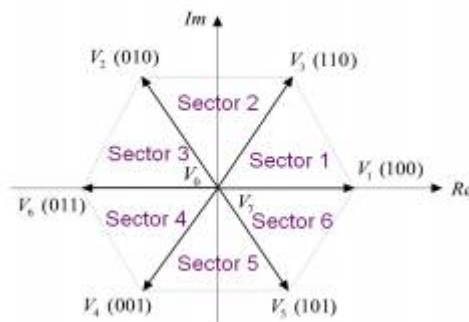


**Fig. 2 The Symmetrical Space Vector PWM Scheme**

### III. COMPARISON OF TOLERANCE CONTROLS

In this section, the characteristics of tolerance controls introduced in Section IV, are analyzed and compared in the simulation results. The simulation circuit is the same as that shown in Fig. 1. For the analysis of the input current ripple, dc-link voltage ripple, and switch losses, simulation parameters are as follows: the rated power is 1.5 kW, the grid line-to-line voltage is 127 Vrms, the grid frequency is 60 Hz, the L-filter value is 1 mH, the dc-link voltage is 200 V, the dc-link capacitor is 1100  $\mu$ F, the load is 33.3  $\Omega$ , the switching frequency is 10 kHz, and the control period is 100  $\mu$ s. The parameters of the insulated gate bipolar mode transistor (IGBT) module 4MBI300VG-120R-50 from Fuji Electric were used in the simulation.

Three tolerance controls restore the distorted input currents after 0.5 s as shown in Fig. 13; however, each tolerance control has a different pole voltage and current ripple is also different. R2LS-TC makes the pole voltage of three-phase as two levels ( $V_{dc}/2$  and  $-V_{dc}/2$ ) as shown in Fig. 13(a). The a-phase pole voltage has two levels in Sectors II and V, and, in the rest of the Sector, the a-phase pole voltage is clamped as  $V_{dc}/2$  and  $-V_{dc}/2$  when 3LSO-TC is applied. The b- and c-phase pole voltages maintain the three levels as shown in Fig. 13(b). OP2LS-TC makes the a-phase pole voltage as two levels in all the Sectors. The b- and c-phases have three-level pole voltages as shown in Fig. 13(c). Fig. 14 shows the expanded current waveforms of tolerance controls. R2LS-TC increases the ripple of three-phase currents in Sectors II-V as shown in Fig. 14(b) owing to

## International Journal of Innovative Research in Science, Engineering and Technology

(An ISO 3297: 2007 Certified Organization)

Vol. 5, Issue 3, March 2016

the 2-LSM.3LSO-TC has current ripple in Sector II–V that is smaller thanthat of R2LS-TC; nevertheless, the current ripple in Sectors Iand IV increases compared with that of R2LS-TC.

The dc-link voltage and the neutral-point voltage(top- and bottom voltages) when each tolerance control isapplied at unity power factor. Among the three tolerance controls,R2LS-TC has smallest ripple in the neutral-point voltage.The neutral-point voltages of 3LSO-TC and OP2LS-TC containlarger ripple. Therefore, the dc-link voltage also has ripple becauseit is affected by the ripple of the neutral-point voltages.Table VI lists the magnitudes of the dc-link voltage and theneutral-point voltage ripple ( $V_{dc,ripple}$  ,  $V_{neu,ripple}$  ), here thepower factor is unity according to various power levels (Load =27, 33, and 66  $\Omega$ ). As a result, R2LS-TC is advantageous in theripple of the dc-link voltage and the neutral-point voltage.

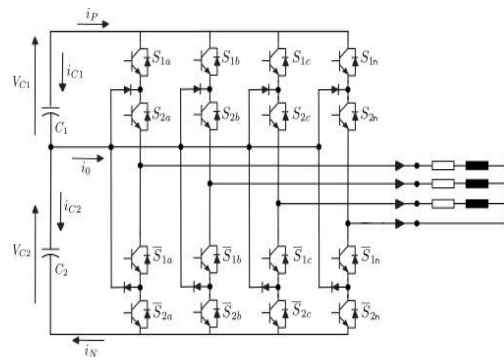


**Fig. 3 Proposed Circuit Diagram**

Switching State	Device Switching Status (Phase A)				Inverter Terminal Voltage $V_{AZ}$
	$S_1$	$S_2$	$S_3$	$S_4$	
P	On	On	Off	Off	$E$
O	Off	On	On	Off	0
N	Off	Off	On	On	$-E$

**Fig. 4 Modes of Operation**

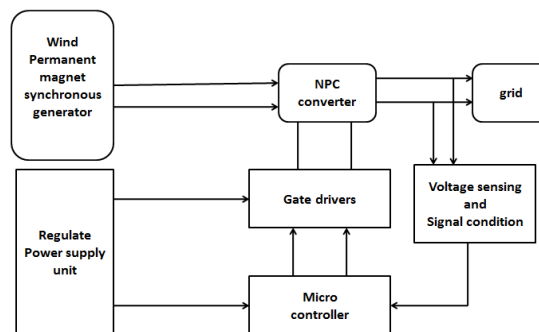


**Fig. 5 Proposed Block Diagram**

# International Journal of Innovative Research in Science, Engineering and Technology

(An ISO 3297: 2007 Certified Organization)

Vol. 5, Issue 3, March 2016

## IV. RESULTS

Open-Switch Fault Detection Method of a Back-to-Back Converter Using NPC Topology for Wind Turbine Systems

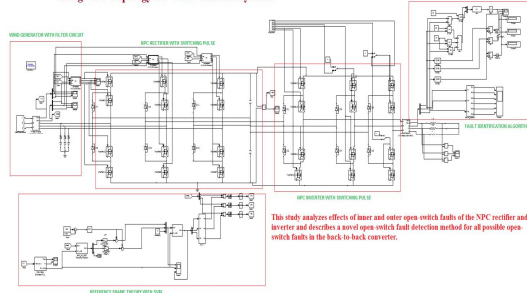


Fig. 6 Proposed Simulink Diagram

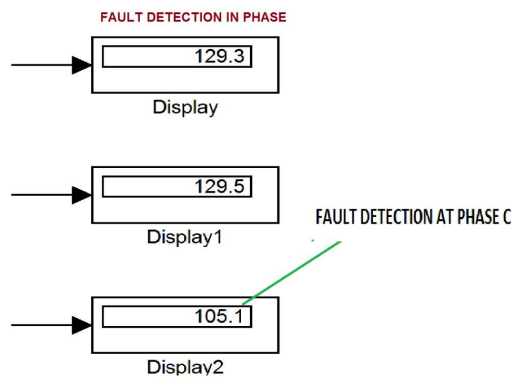


Fig. 7 Fault Detection

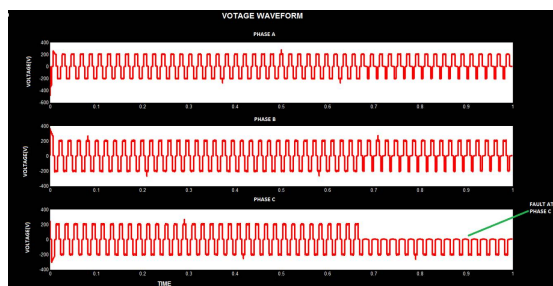


Fig. 8 Output Voltage

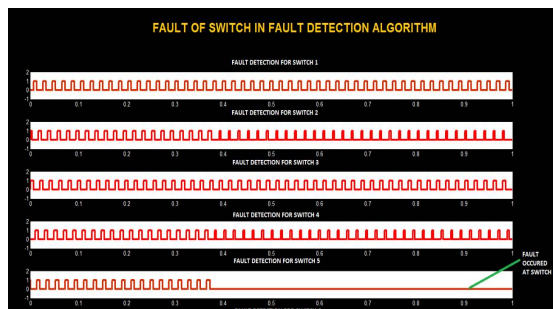
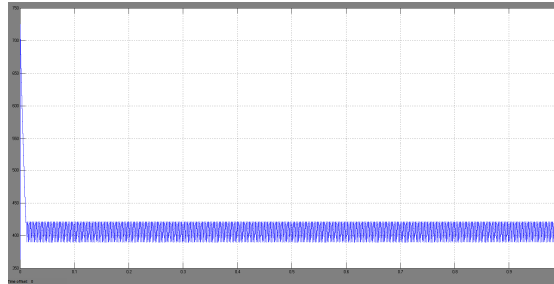
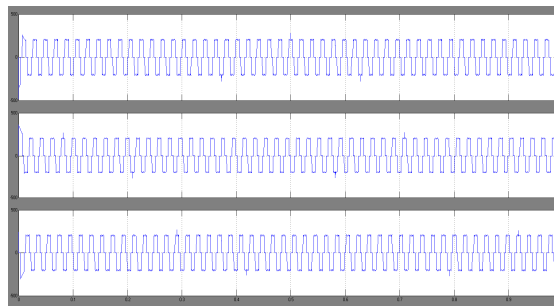


Fig. 9 Fault of Switch in Fault Detection Algorithm



**Fig. 10 Output for DC link Voltage**



**Fig. 11 Output Voltage**

Since the microcontroller is a digital device, it is mandatory to supply +5V DC supply. The supply from the battery or the AC supply are to be regulated to +5V DC in order to feed the microcontroller.

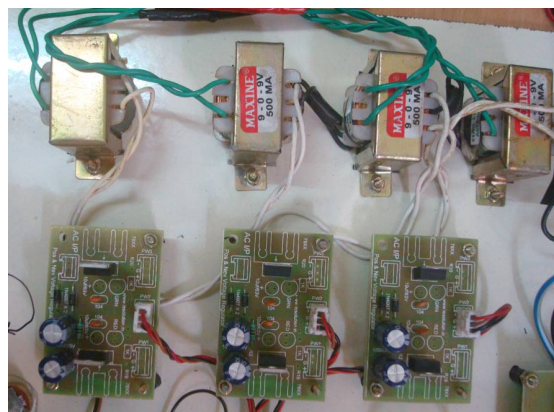


**Fig. 12 Proposed Hardware**

## V. CONCLUSION

This paper proposed a three-level switching-oriented (3LSO) tolerance control for the T-type rectifier and analyzed the characteristic of the tolerance control by comparing it with that of the two tolerance controls. The introduced tolerance controls were described in terms of the space vector and characteristics were identified by using simulation and experimental results. Additionally, to evaluate these controls, following three factors were considered: the current THD, dc-link voltage ripple, and efficiency. From analyzed results, we arrived at the following conclusion:

R2LS-TC: This control guarantees the lower dc-link voltage ripple compared to the other tolerance controls (3LSO-TC and OP2LS-TC). In sectors that operate as the conventional three-level switching method, the neutral-point voltage balancing control can be conducted; however, it causes the current THD and efficiency to be high and low.



# International Journal of Innovative Research in Science, Engineering and Technology

(An ISO 3297: 2007 Certified Organization)

Vol. 5, Issue 3, March 2016

3LSO-TC: This control guarantees higher efficiency. Still the current THD and the dc-link voltage ripple increase. Additionally, the changed small vectors from infeasible vectors due to the open-switch fault are not used for the neutral-point voltage balancing control; however, the changed vectors for neutral-point voltage balancing control in opposite sectors can be used to the neutral-point voltage balancing control (the small vectors, which is the opposite type, in the opposite sectors guarantee the neutral-point balance). These vectors for neutral-point voltage balancing control are decided depending on the position of the open-switch fault; therefore, the neutral-point voltage balancing control in 3LSO-TC has a limitation.

Consequently, these tolerance controls have different advantages, and they should be selected by considering the specific requirements of applications using the T-type rectifier.

## REFERENCES

- [1] F. Xu, B. Guo, L. M. Tolbert, F. Wang, and B. J. Blalock, "An all-SiC three-phase buck rectifier for high-efficiency data center power supplies," *IEEE Trans. Ind. Appl.*, vol. 49, no. 6, pp. 2662–2673, Nov./Dec. 2013.
- [2] H. S. Kim, J. W. Baek, M. H. Ryu, J. H. Kim, and J. H. Jung, "The high efficiency isolated AC–DC converter using the three-phase interleaved LLC resonant converter employing the Y-connected rectifier," *IEEE Trans. Power Electron.*, vol. 29, no. 8, pp. 4017–4028, Aug. 2014.
- [3] K. Ma, F. Blaabjerg, and M. Liserre, "Thermal analysis of multilevel grid-side converters for 10-MW wind turbines under low-voltage ride through," *IEEE Trans. Ind. Appl.*, vol. 49, no. 2, pp. 708–719, Mar./Apr. 2013.
- [4] R. C. Portillo, M. M. Prats, J. I. Leon, J. A. Sánchez, J. M. Carrasco, E. Galvan, and L. G. Franquelo, "Modeling strategy for back-to-back three-level converter applied to high-power wind turbines," *IEEE Trans. Ind. Electron.*, vol. 53, no. 5, pp. 1483–1491, Oct. 2006.
- [5] Y. S. Park, S. K. Sul, and C. H. Lim, "Asymmetric control of DC-link voltages for separated MPPTs in three-level inverters," *IEEE Trans. Power Electron.*, vol. 28, no. 6, pp. 2760–2769, Jun. 2013.
- [6] S. Alepuz, A. Calle, S. Busquets-Monge, S. Kouro, and B. Wu, "Use of stored energy in PMSG rotor inertia for low-voltage ride-through in back-to-back NPC converter-based wind power systems," *IEEE Trans. Ind. Electron.*, vol. 60, no. 5, pp. 1787–1796, May 2013.
- [7] L. Hang, M. Zhang, L. M. Tolbert, and Z. Lu, "Digitized feedforward compensation method for high-power-density three-phase Vienna PFC converter," *IEEE Trans. Ind. Electron.*, vol. 60, no. 4, pp. 1512–1519, Apr. 2013.
- [8] J. D. Barros, J. F. A. Silva, and E. G. A. Jesus, "Fast-predictive optimal control of NPC multilevel converters," *IEEE Trans. Ind. Electron.*, vol. 60, no. 2, pp. 619–627, Feb. 2013.
- [9] J. S. Lee and K. B. Lee, "New modulation techniques for a leakage current reduction and a neutral-point voltage balance in transformerless photovoltaic systems using a three-level inverter," *IEEE Trans. Power Electron.*, vol. 29, no. 4, pp. 1720–1732, Apr. 2014.
- [10] A. Sanchez-Ruiz, M. Mazuela, S. Alvarez, G. Abad, and I. Baraia, "Medium voltage–high power converter topologies comparison procedure, for a 6.6 kV drive application using 4.5 kV IGBT modules," *IEEE Trans. Ind. Electron.*, vol. 59, no. 3, pp. 1462–1476, Mar. 2012.
- [11] H. J. Shin and J. I. Ha, "Phase current reconstructions from DC-link currents in three-phase three-level PWM inverters," *IEEE Trans. Power Electron.*, vol. 29, no. 2, pp. 582–593, Feb. 2014.
- [12] Y. Zhang, J. Zhu, Z. Zhao, W. Xu, and D. G. Dorrell, "An improved direct torque control for three-level inverter-fed induction motor sensorless drive," *IEEE Trans. Power Electron.*, vol. 27, no. 3, pp. 1502–1513, Mar. 2012.